

Electrical Properties of Amorphous InSb

J. J. Hauser

Bell Laboratories, Murray Hill, New Jersey 07974

(Received 24 January 1973)

Amorphous InSb films were prepared by getter sputtering on substrates held at 77 °K and at room temperature. The films prepared at 300 °K are very similar to films evaporated at lower temperatures: Their resistivity increases exponentially with decreasing temperature (intrinsic conduction) with an electrical band gap E_g^{cl} of about 0.5 eV. On the other hand, films deposited and kept at 77 °K have a temperature-dependent resistivity which is well fitted between 10 and 120 °K by the relation $\rho = \rho_0 \exp[(T_0/T)^{1/4}]$, with $T_0 \simeq 2 \times 10^7$ °K, thus suggesting that conduction in such films takes place via a thermally activated hopping mechanism. Above 120 °K the films anneal as shown by the increasing resistivity with increasing temperature; after annealing the films display again an exponentially temperature-dependent resistivity similar to that of a room-temperature-deposited film. InSb is therefore an interesting amorphous semiconductor from the point of view that either intrinsic or hopping conduction over most of the accessible temperature range can be achieved by varying the conditions of deposition; this suggests that the localized states between which electrons are hopping in the films deposited at 77 °K may be linked with the greater degree of disorder present in such films.

I. INTRODUCTION

Eckenbach, Fuhs, and Stuke¹ (EFS) reported the preparation of amorphous InSb films by vapor deposition onto substrates, the temperatures of which ranged between 150 and 200 °K (some films were deposited at 90 °K which displayed strange annealing behaviors and broke at higher temperatures). In all cases the thin films were characterized by an exponential dependence of the conductivity on $1/T$ with a large activation energy E_g^{cl} ranging between 0.4 and 0.65 eV. In general,² the temperature dependence of the electrical conductivity in most amorphous compounds and alloys is exponential with a single activation energy. In contrast, elemental amorphous films of Ge,^{3,4} Si,^{5,6} Te,⁷ and C^{8,9} always display at low temperatures a dependence with a continuously diminishing activation energy: The temperature dependence of the resistivity of Ge^{3,4,10} and Si^{5,6,11} can be fitted between room temperature and 30 °K by the relation^{12,13}

$$\rho = \rho_0 e^{(T_0/T)^{1/4}}, \quad (1)$$

where¹³ $kT_0 = 16\alpha^3/N(E_F)$, k is Boltzmann's constant, α is the coefficient of exponential decay of localized states, and $N(E_F)$ is the density of localized states. At high enough temperatures, conduction becomes intrinsic² unless crystallization or other structural changes intervene. This intrinsic behavior is, however, restricted to a fairly narrow temperature range and one may always question whether this intrinsic behavior is not caused in part by microcrystallization undetectable by x-ray and electron diffraction. On the other hand, it has been shown for Ge¹⁰ and Si,¹¹ that while the resistivity is always well represented by relation (1), one can increase the number of localized states

(as evidenced by the decrease in T_0) by sputtering the films at 77 °K. It seems that the increase in the number of localized states is linked to a greater degree of disorder^{10,11} caused both by the sputtering process and by the low temperature of deposition. It would therefore be interesting to find out whether one could change the intrinsic conduction observed in InSb by EFS¹ to the hopping conduction represented by relation (1) by simply increasing the degree of disorder of the films. This study will therefore concentrate on InSb films sputtered at 77 °K.

II. EXPERIMENTAL PROCEDURE

The films were deposited on sapphire and glass substrates by getter sputtering¹⁴ from an InSb target. The InSb target was prepared¹⁵ by inductively melting and stirring several times an InSb charge inside a graphite mold. The composition of the target was checked by x-ray fluorescence analysis and the structure of the target was established by x-ray diffraction. The rates of deposition varied between 45 and 70 Å/min, the low rates being necessary to maintain a temperature of deposition of 77 °K. For the transverse-electrical-resistance measurements, the InSb films were deposited between two narrow orthogonal Pb electrodes with a cross-sectional area of 3.6×10^{-4} cm². This geometry allows four-probe resistance measurements which eliminates the necessity for electrode-resistance corrections. Furthermore, the deposition of both electrodes (by evaporation) and InSb films at 77 °K without either breaking the vacuum or raising the temperature eliminated the formation of an oxide barrier. For both planar and transverse measurements, films deposited at 77 °K were transferred onto a holder without warming and the resis-

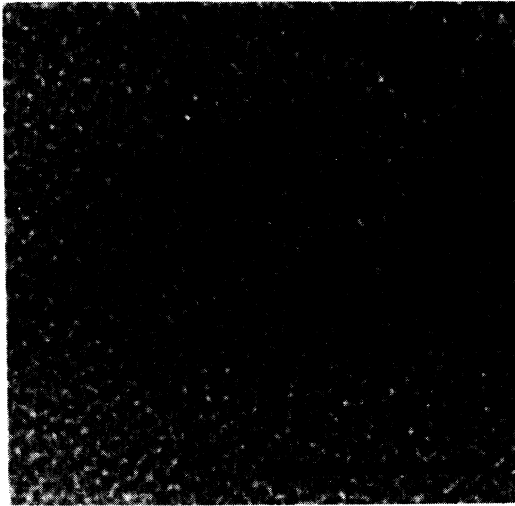


FIG. 1. Underfocused bright-field electron micrograph for a 100-Å InSb film deposited at room temperature on a NaCl substrate.

tivity was measured at first by cooling down (to 1 °K if so desired) and then by warming up above 77 °K to study the annealing behavior of the films. Some films were deposited at room temperature at the same rate as films deposited at 77 °K. All resistance measurements, planar and transverse, are low-field measurements and were obtained with electrical fields smaller than 10^2 V/cm. The electron micrograph and electron diffractions were obtained¹⁶ by depositing a 100-Å film onto a cleaned NaCl substrate. The film was then floated free and mounted on a holey carbon substrate and examined by high-resolution electron microscopy (magnification 250 000) with an underfocusing of about 3000 Å. For films deposited at 77 °K, the x-ray diffractometer trace was obtained at 77 °K without warming up the film.

III. EXPERIMENTAL RESULTS AND DISCUSSION

The room-temperature x-ray diffraction of a film deposited at 300 °K is in excellent agreement with the electron diffraction reported by EFS¹: There are two broad peaks, the [111] being close to the crystalline value, while there is a broad peak which replaces InSb [220] and InSb [311]; the broad peak between InSb [311] and InSb [422] reported by EFS¹ could not be resolved in the present experiments. The amorphous x-ray diffraction pattern is very similar qualitatively to those of amorphous Ge^{10,17} and Si.¹¹ Furthermore, similar to amorphous Ge,¹¹ one finds that the x-ray diffraction taken at 77 °K on a film deposited and kept at 77 °K displays an even more distorted amorphous structure as revealed by still broader diffraction peaks. The electron transmission micrograph for an amorphous

film deposited at 300 °K is shown in Fig. 1. It is interesting to note that Fig. 1 shows a defect structure similar to the one reported for Ge^{10,17} and Si,¹¹ i. e., dark areas surrounded by a network of density-deficient channels (cracks?). This would suggest that the crack network is not the result of the tetrahedral bonding of Ge and Si but rather a result of the brittle nature of these amorphous semiconductors. While amorphous InSb films could only be obtained by low-temperature evaporation,¹ it was found that, as shown by x-ray and electron diffraction [Fig. 2(a)], one may sputter amorphous InSb films at room temperature. On the other hand, as shown in Fig. 2(b), where another region of the film was investigated, it is clear that although the film is amorphous, partial microcrystallization is present as well. Consequently, unless a film is deposited at 77 °K, one should consider the possibility of microcrystals embedded in the amorphous matrix. It is therefore possible that microcrystallization was present in the films deposited by EFS.¹ The microcrystallization was not evident in their electron diffraction¹ either because the amount was less than in films sputtered at 300 °K or because it was missed by insufficient scanning [Fig. 2(a) vs Fig. 2(b)].

Turning our attention to the electrical properties of amorphous InSb, we shall first consider films deposited and kept at 77 °K until measured. The temperature dependence of the resistance measured in the plane of the film for such films is shown in Figs. 3 and 4. The electrical as well as other physical properties for the films of the present study are summarized in Table I. It is obvious from Figs. 3 and 4 that the resistivity for films deposited at 77 °K can be fitted quite well by relation (1) between 10 and 90 °K with $T_0 \approx 2 \times 10^7$ °K. This value of T_0 seems independent of thickness within a factor of 2 for films ranging in thickness between 1000 Å and 1.4 μm and has the same order of magnitude as that reported for amorphous Ge ($T_0 \approx 10^8$ °K)^{3,18} and for amorphous Si ($T_0 \approx 6 \times 10^7$ °K).^{5,6} The value of T_0 is higher for the 310-Å film in

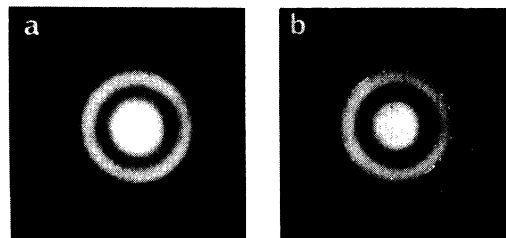


FIG. 2. Electron diffractions taken on different regions of the same film of which the electron micrograph is shown in Fig. 1: (a) totally amorphous pattern; (b) amorphous pattern with partial microcrystallization.

TABLE I. Properties of InSb films.

Film	$d_{\text{InSb}}(\text{\AA})$	$T_D(^{\circ}\text{K})^a$	$\sigma_{\text{RT}}(\Omega^{-1} \text{cm}^{-1})^b$	$T_0(^{\circ}\text{K})$	$E_g^{e1}(\text{eV})$
InSb No. 1	6000	77	4.4	2.5×10^7	...
InSb No. 1 warmed up to 300 °K			0.03
InSb No. 2	13 800	77	2.9	3.8×10^7	...
InSb No. 3	7430	77	5.4	1.2×10^7	...
InSb No. 3 annealed ^c 16 h			0.0013	...	0.5
InSb No. 6	1875	77	8	1.9×10^7	...
InSb No. 6 warmed up to 300 °K			0.0048	...	0.5
InSb No. 6 annealed ^c 48 h			0.0007	...	0.58
InSb No. 5	310	77	5.8	8.4×10^7	...
InSb No. 5 annealed ^c 16 h			0.0012	...	0.93
InSb No. 9	2100	77	7.6	2.7×10^7	...
InSb No. 7	30 000	77	6.5	2.8×10^3	0.036
InSb No. 4	8290	300	0.55	...	0.38
InSb No. 10	13 400	300	0.13	...	0.39
Pb-InSb-Pb No. 1	10 800	77	1.0(1.0) ^d	7.5×10^6	0.042
Pb-InSb-Pb No. 3	5400	77	1.5(0.4) ^d	7.5×10^6	0.038
Pb-InSb-Pb No. 4	5400	77	6(0.4) ^d	1.25×10^7	0.038
Pb-InSb-Pb No. 5	6300	77	1.2(1.2) ^d	1.4×10^7	0.056
Pb-InSb-Pb No. 5 annealed ^c 16 h			0.058	...	0.5

^a T_D is the temperature of deposition of the film.

^bThis is the room-temperature conductivity for a film deposited or annealed at 300 °K, it is $\sigma_{\text{extr RT}}$ for films deposited at 77 °K (see text).

^cThe anneal, unless otherwise indicated, was performed at 300 °K.

^dThese values were obtained by extrapolation to room temperature of the exponential plot shown in Fig. 9, while the other values were extrapolated from the $T^{-1/4}$ plot of Fig. 8.

agreement with the increase in T_0 observed for very thin films in both Ge¹⁹ and Si.¹¹ This increase in T_0 was attributed¹⁹ either to the changing defect structure of such thin films or to the fact that at low temperatures the electron hopping distance becomes limited by the film thickness.²⁰ One can see from Figs. 3 and 4 that the films anneal around 90 °K as shown by the deviation from the low-temperature data towards higher resistance. If one extrapolates the low-temperature data to room temperature one obtains a conductivity $\sigma_{\text{extr RT}}$ on the order of a few $\Omega^{-1} \text{cm}^{-1}$ which is higher than the value for room-temperature-deposited films or for films annealed at room temperature (see Table I).

One also notes the very different annealing behaviors of the films sputtered at 77 °K and those evaporated at 90 °K.¹ EFS reported¹ a reversible curve above 90 °K with a small positive temperature coefficient followed by two irreversible processes near 200 °K, one leading to an increase and the other to a large irreversible decrease in σ . On the other hand, the films sputtered at 77 °K have a simple annealing behavior similar to the one reported^{10,19} for Ge films sputtered at 77 °K. Indeed, one observes only an irreversible decrease in con-

ductivity above the annealing temperature of 90 °K (120 °K for Ge). However, after a room-temperature anneal one observes an exponential temperature dependence of the conductivity which, except for minor differences, is in good agreement with that observed by EFS.

Leaving aside InSb No. 5 which displays a very large energy gap (0.93 eV) possibly caused by its small thickness (Fig. 3), one observed in Fig. 4 that the annealed films can be fitted between 300 and 140 °K by a single energy gap of about 0.5 eV. This differs slightly from EFS who reported approximately the same energy gap for the intrinsic region at high temperature, but observed an extrinsic region with lower energy gap at low temperatures. Although many factors may be responsible for such a difference, we would like to suggest that the extrinsic region in the evaporated films is the result of microcrystallization which, as discussed above, may not always be detected in the electron-diffraction pattern. Such microcrystallization would be absent in the films sputtered at 77 °K as suggested by the more distorted nature of the x-ray pattern. Furthermore, as previously discussed, even in films sputtered at room temperature, the

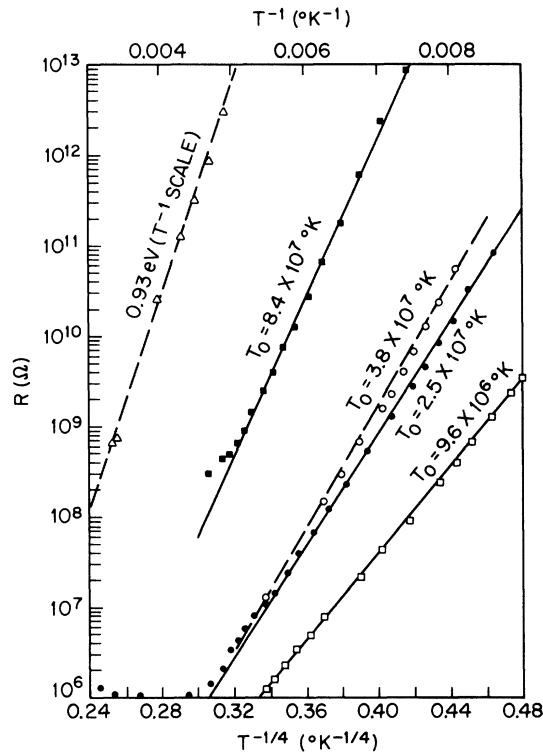


FIG. 3. Temperature dependence of the planar resistance for films deposited at 77°K; all film resistances are plotted vs $T^{-1/4}$ except for the annealed InSb No. 5 film which is plotted vs T^{-1} . Closed dot (●), InSb No. 1, 6000 Å; open dot (○), InSb No. 2, 1.4 μm; open square (□), InSb No. 3, 7430 Å; InSb No. 5, 310 Å, closed square (■) as deposited, open triangle (Δ) annealed 16 h at 300°K.

microcrystallization does not occur uniformly in the film and may easily be missed. Consequently, the conductivity-versus-temperature curve for a film consisting of microcrystals embedded in an amorphous matrix will consist of the superposition of the curve for an amorphous material with a single energy gap and of the curve for the crystalline material¹ which saturates around 200°K. This superposition will give rise to a temperature-dependent conductivity with two energy gaps. This suggestion is supported by the data shown in Fig. 5 for two films sputtered at room temperature where microcrystallization is present as shown by Fig. 2(b): The energy gaps correspond to the low values reported by EFS and we can observe an intrinsic region at high temperature followed by an extrinsic region at low temperature. The data for films deposited at 77°K and annealed at 300°K, as well as for films deposited at 300°K, are shown in Fig. 6, where they are compared with the data of EFS. The qualitative agreement between the various data is satisfactory. The temperature dependence of the transverse conductivity has been in-

cluded in Fig. 6 and is in good agreement with the planar temperature dependence; this point will be further discussed, later on, with the transverse measurements. One further point of agreement with EFS is that the electrical energy gap increases upon annealing: E_g^{el} increases from 0.5 to 0.58 eV after an anneal of 48 h at room temperature (see the data for InSb No. 6 in Fig. 4). These results are summarized as follows: Films sputtered at 77°K display a hopping conduction with $\sigma \propto T^{-1/4}$, where the localized states are the result of the disorder caused by the low temperature of deposition and the sputtering process; upon annealing at room temperature, the localized states are removed and one observes an exponential temperature dependence with a single energy gap. Films deposited at room temperature display an exponential temperature dependence with two energy gaps (intrinsic and extrinsic regions) possibly because such films have

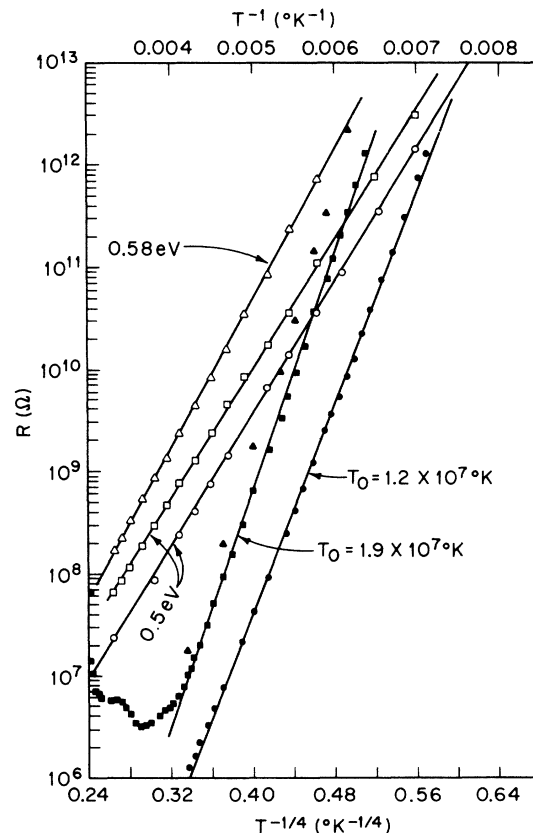


FIG. 4. Temperature dependence of the planar resistance for films deposited at 77°K showing the effect of room-temperature annealing. InSb No. 3, 7430 Å, closed dot (●) $T^{-1/4}$ scale, as deposited, open dot (○) T^{-1} scale, annealed 16 h; InSb No. 6, 1875 Å, closed square (■) $T^{-1/4}$ scale, as deposited, open square (□) T^{-1} scale, after warm up to 300°K, open triangle (Δ) T^{-1} scale, annealed 48 h; InSb No. 9, 2100 Å, $T^{-1/4}$ scale [only a few closed triangles (▲) indicated].

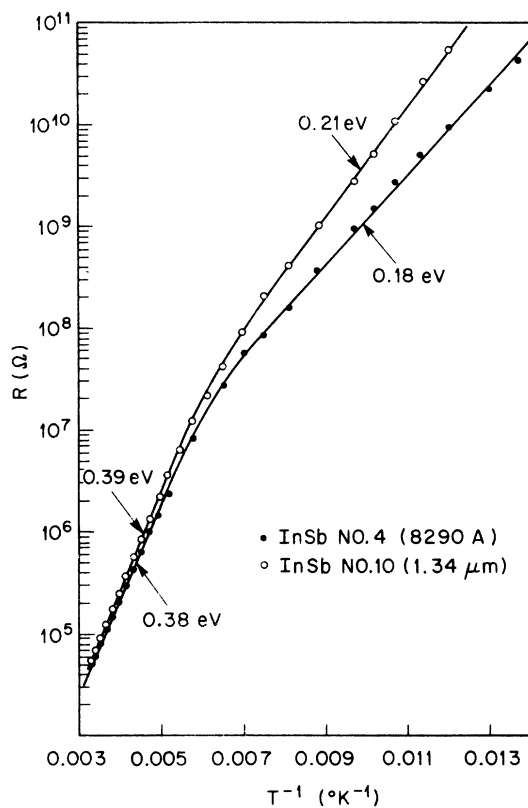


FIG. 5. Temperature dependence of the planar resistance for two films sputtered at room temperature.

a similar structure to the evaporated films.¹ Indeed, extrinsic conductivity occurring as a result of annealing has been previously observed in amorphous chalcogenide films.²¹

Another interesting parameter in such films is the number of carriers. Although the Hall voltage on InSb No. 10 was too small to be detected, one could estimate at room temperature a useful lower limit for the Hall constant: $R \leq 0.7 \text{ cm}^3/\text{C}$; this corresponds to a density of carriers of at least $9 \times 10^{18} \text{ cm}^{-3}$ with an associated mobility smaller than $0.1 \text{ cm}^2/\text{V sec}$. These numbers are in good agreement with Clark's Hall-effect measurements⁴ on amorphous Ge. Furthermore, as Stuke²² has suggested that the product of the density of states times the mobility is a constant for both amorphous and crystalline semiconductors with a given energy gap, one finds again that the high density of carriers of amorphous films is linked to a very low mobility. In the case where conduction is via hopping between localized states, one can calculate the density of localized states from the relation previously mentioned: Using $T_0 \approx 2 \times 10^7 \text{ °K}$ and¹³ $\alpha \approx 10^7 \text{ cm}^{-1}$ one obtains $N(E_F) \approx 10^{19} \text{ cm}^{-3}$, which is of the same order of magnitude as the estimated number of extended states.

It is already clear that it is more difficult to obtain InSb in the amorphous state than Ge and Si. Indeed, while EFS state¹ that amorphous InSb films had to be evaporated at low temperature, amorphous Ge films can be evaporated at temperatures as high as 300 °C .¹⁷ The readiness of InSb to revert to the crystalline state is further demonstrated by the effect of film thickness on the crystalline state of the film. While films thinner than 1.5 μm are amorphous, thicker films, although amorphous from their x-ray diffraction pattern, show clear evidence of microcrystallinity in their electrical behavior. This effect is shown in Fig. 7 for a 3-μm film deposited at 77 °K . The best evidence for microcrystallinity is the very high conductivity of the film (see Table I) coupled with the fact that although the film was deposited at 77 °K , the resistance-versus-temperature curve is totally reversible between

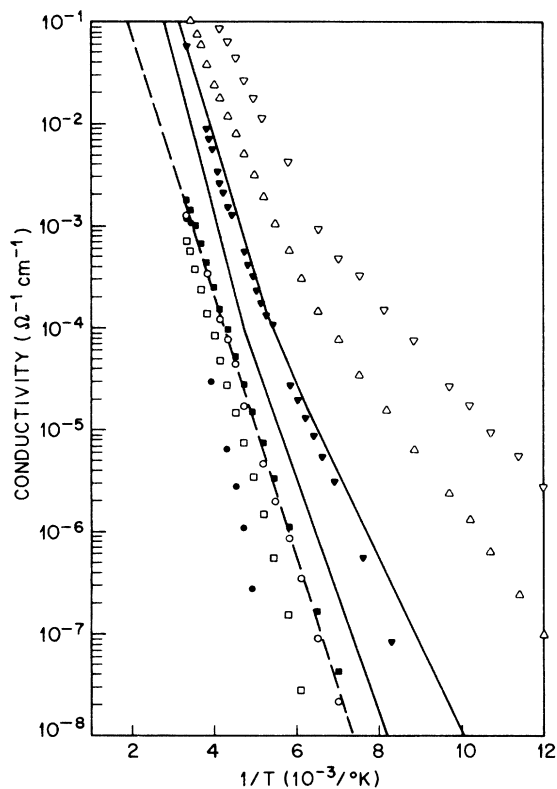


FIG. 6. Conductivity vs reciprocal temperature for films deposited at 77 °K and annealed at 300 °K and for films deposited at 300 °K . InSb No. 5, 310 Å , annealed 16 h closed dot (●); InSb No. 6, 1875 Å , closed square (■) cooled from 300 °K , open square (□) annealed 48 h; InSb No. 3, 7430 Å , annealed 16 h, open dot (○); InSb No. 4, 8300 Å , deposited at 300 °K , open inverted triangle (▽); InSb No. 10, 1.34 μm , deposited at 300 °K , open triangle (Δ); Pb-InSb-Pb No. 5, 6300 Å , annealed 16 h, closed inverted triangle (▼). The two solid lines represent the amorphous data shown in Fig. 4 by EFS (Ref. 1).

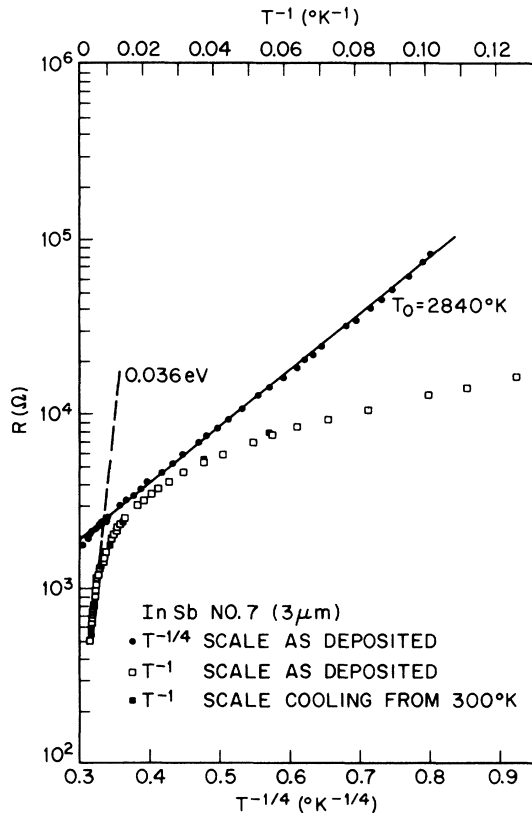


FIG. 7. Temperature dependence of the planar resistance for 3- μm film deposited at 77°K.

2.5 and 300°K. Furthermore, although the data below 110°K can still be fitted by relation (1), T_0 is extremely low (2.8×10^3 °K), and above 110°K the temperature dependence of the resistance becomes exponential, but with a very small energy gap (0.036 eV). All these facts can be best explained in terms of microcrystals (too small to be detected by x-ray diffraction) embedded in an amorphous matrix. This microcrystalline behavior seems to develop at a film thickness of approximately 2 μm .

We now turn our attention to the temperature dependence of the transverse resistance for films deposited, and kept, at 77°K (Figs. 8 and 9). While in amorphous Ge films¹⁰ the planar and transverse resistances were both proportional to $T^{-1/4}$ up to the annealing temperature of 120°K, this is not the case for InSb as shown by Fig. 8. The data can be fitted by relation (1) with $T_0 \approx 10^7$ °K (Table I) below 20°K, but above 20°K up to the annealing temperature of 90°K the data are best fitted by an exponential with a very small activation energy of 0.05 eV (Fig. 9). The different temperature dependence between planar and transverse measurements cannot be explained in terms of anisotropy as over the whole range of temperatures studied; the transverse resistivity values are, within scat-

ter, approximately equal to the planar resistivity values. Furthermore, the film thickness studied in the transverse measurements is too thick to expect any anisotropy.^{10,11} The different temperature dependence between planar and transverse resistance measurements can be explained by the different degree of disorder between the two types of films. While the films for planar measurements are deposited on glass or sapphire, the films for the transverse measurements are deposited on an evaporated Pb film. One may therefore expect²³ that the films grown on Pb will be less disordered, and as a result, the exponential dependence with the small activation energy can be considered as a transitional state between the fully disordered state ($\sigma \propto T^{-1/4}$) and the fully annealed state [$\sigma \propto \exp(-E_g^{e1}/kT)$, with $E_g^{e1} \approx 0.5$ eV]. On the other hand, these differences are not that important if considered in the following way: Both $T_0 (\approx 10^7$ °K) and the value of $\sigma_{\text{extr RT}}$ extrapolated from the $T^{-1/4}$ plot of

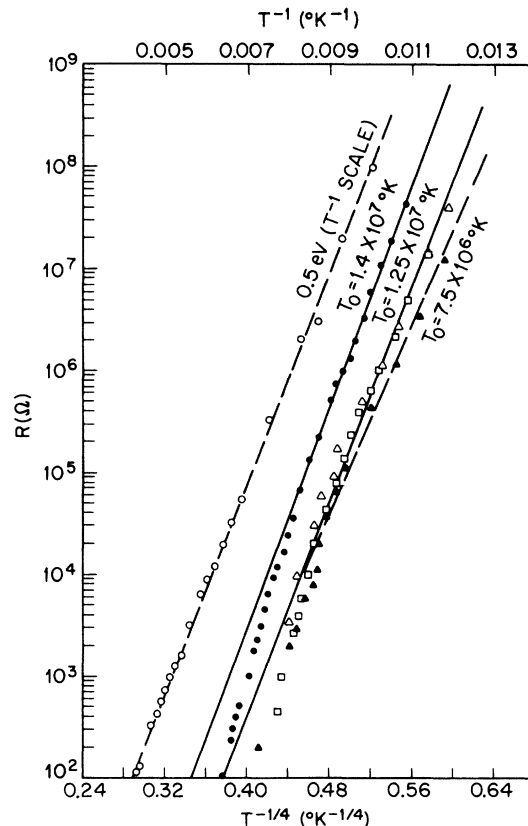


FIG. 8. Temperature dependence of the transverse resistance for films deposited at 77°K; all film resistances are plotted vs $T^{-1/4}$ except for the annealed Pb-InSb-Pb No. 5 film which is plotted vs T^{-1} . Pb-InSb-Pb No. 1, 1.1 μm , open triangle (Δ); Pb-InSb-Pb No. 3, 5400 Å, closed triangle (\blacktriangle); Pb-InSb-Pb No. 4, 5400 Å, open square (\square); Pb-InSb-Pb No. 5, 6340 Å, closed dot (\bullet) as deposited, open dot (\circ) annealed 16 h.

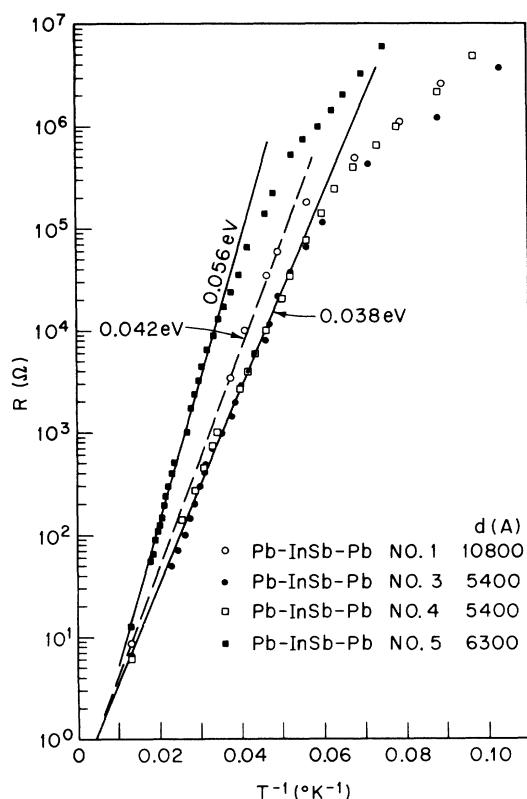


FIG. 9. Transverse resistance for the same films described in Fig. 8 as a function of reciprocal temperature. Pb-InSb-Pb No. 1, open dot (○); Pb-InSb-Pb No. 3, closed dot (●); Pb-InSb-Pb No. 4, open square (□); Pb-InSb-Pb No. 5, closed square (■).

Fig. 8 (a few $\Omega^{-1} \text{cm}^{-1}$) are very close to the values obtained for the planar measurement (Table I). Furthermore, if one obtains $\sigma_{\text{extr RT}}$ from the T^{-1} plot of Fig. 9, the resulting values are still fairly close (except for Pb-InSb-Pb No. 4) to those obtained from the $T^{-1/4}$ extrapolation and are still much larger than the room-temperature conductivity of annealed films. As shown in Fig. 8, the temperature dependence of the transverse resistance for a film annealed at room temperature is in very good agreement with planar measurements ($E_g^{\text{pl}} = 0.5 \text{ eV}$). These data are also shown in Fig. 6, where one can see that they are in excellent agreement with the data of EFS.¹ One also notes in Fig. 6 that while planar measurements are fitted with a single activation energy, the transverse measurements show both an intrinsic and an extrinsic region. As mentioned above, this difference can be understood in terms of partial microcrystallization present in annealed films deposited for transverse measurements: In other words, a film deposited at 77°K on a metal substrate (Pb) and subsequently annealed partially crystallizes, just as a film deposited on glass or sapphire at 300°K.

ACKNOWLEDGMENTS

I would like to thank J. E. Bernardini, Miss A. Staudinger, and D. Dorsi for their technical assistance. I am also thankful to L. R. Testardi for discussions and suggestions on the Hall effect.

¹ W. Eckenbach, W. Fuhs, and J. Stuke, *J. Non-Cryst. Solids* **5**, 264 (1971).
² R. Grigorivici, *Thin Solid Films* **9**, 1 (1971).
³ P. A. Walley and A. K. Jonscher, *Thin Solid Films* **1**, 367 (1967).
⁴ A. H. Clark, *Phys. Rev.* **154**, 750 (1967).
⁵ P. A. Walley, *Thin Solid Films* **2**, 327 (1968).
⁶ M. Morgan and P. A. Walley, *Philos. Mag.* **23**, 661 (1971).
⁷ H. Keller and J. Stuke, *Phys. Status Solidi* **8**, 831 (1965).
⁸ C. J. Adkins, S. M. Freake, and E. M. Hamilton, *Philos. Mag.* **22**, 175 (1970).
⁹ M. Morgan, *Thin Solid Films* **7**, 313 (1971).
¹⁰ J. J. Hauser, *Phys. Rev. Lett.* **29**, 476 (1972).
¹¹ J. J. Hauser, *Phys. Rev. B* (to be published).
¹² N. F. Mott, *Philos. Mag.* **19**, 835 (1969).
¹³ V. Ambegaokar, B. I. Halperin, and J. S. Langer, *Phys. Rev.*

B **4**, 2612 (1972).
¹⁴ H. C. Theuerer and J. J. Hauser, *J. Appl. Phys.* **35**, 554 (1964).
¹⁵ I am indebted to D. Dorsi for the preparation of the InSb target.
¹⁶ I am indebted to Miss A. Staudinger for the electron micrograph and the electron diffractions shown in Figs. 1 and 2.
¹⁷ T. M. Donovan and K. Heinemann, *Phys. Rev. Lett.* **27**, 1794 (1971).
¹⁸ K. L. Chopra and S. K. Bahl, *Phys. Rev. B* **1**, 2545 (1970).
¹⁹ J. J. Hauser and A. Staudinger, *Phys. Rev. B* **8**, 607 (1973).
²⁰ V. K. S. Shante, *Phys. Lett.* **43A**, 249 (1973).
²¹ E. A. Fagen and H. Fritzsche, *J. Non-Cryst. Solids* **2**, 180 (1970).
²² J. Stuke, *J. Non-Cryst. Solids* **4**, 1 (1970).
²³ J. R. Bosnell and U. C. Voisey, *Thin Solid Films* **6**, 161 (1970).

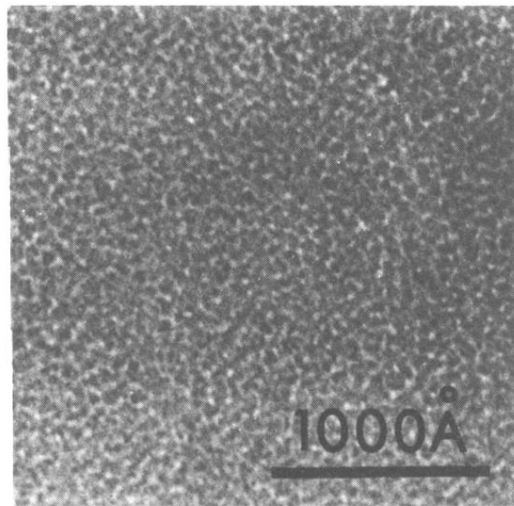


FIG. 1. Underfocused bright-field electron micrograph for a 100-Å InSb film deposited at room temperature on a NaCl substrate.

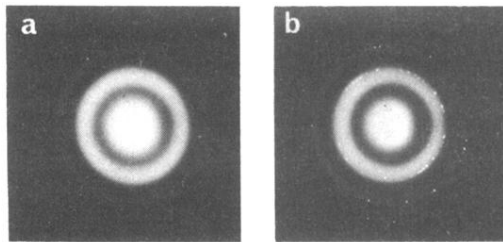


FIG. 2. Electron diffractions taken on different regions of the same film of which the electron micrograph is shown in Fig. 1: (a) totally amorphous pattern; (b) amorphous pattern with partial microcrystallization.